Optimisation of a multi surrogate model system with the help of Genetic algorithm.

Anshuman Sinha[1], Amarendra K Singh[2*]
1,2 Department of Materials Engineering, IIT Kanpur, Kanpur 208016, UP, INDIA
*email: amarendra@iitk.ac.in

AIM: What is the message you wish to convey?

- Creation of Deep learning based surrogate model of physical system from full CFD model, such that online application is made possible
- Optimisation of a multi surrogate model system with the help of Genetic algorithm.

A. Abstract: In an integrated steel mill, duration of BOF operations has gradually reduced on account of improved automation and control. At the same time, productivity of continuous casting machines is improving. Steel specifications are gradually becoming more and more stringent and LF operation contributes majorly in meeting those specifications. For example, the demand for lower sulphur and oxygen levels increases LF processing time. The present study looks at the challenges associated with the ladle furnace operation and explores ways and means of reducing the LF processing time. The present requirement of good quality steel in competition with the productivity requirements, envisage the optimisation of ladle refining processes. In the current work this objective is achieved with the help of surrogate models, that are beneficial in order to reduce the computation time in order to get a handle on dynamic ladle processing while the process is taking place. Surrogate modes are miniature or low-level models that are built on basic physics of the system and mainly rely upon the input-output data of a complete model or actual plant trials. Thorough these data an ML-based or an ANN model is formulated using a close loop predictor-corrector algorithm. The training has been achieved with the help of CFD based model's data from previous publication. The validation of the model is done through data with the help of experimental data from Tata Steel and Medhani Steel plant.

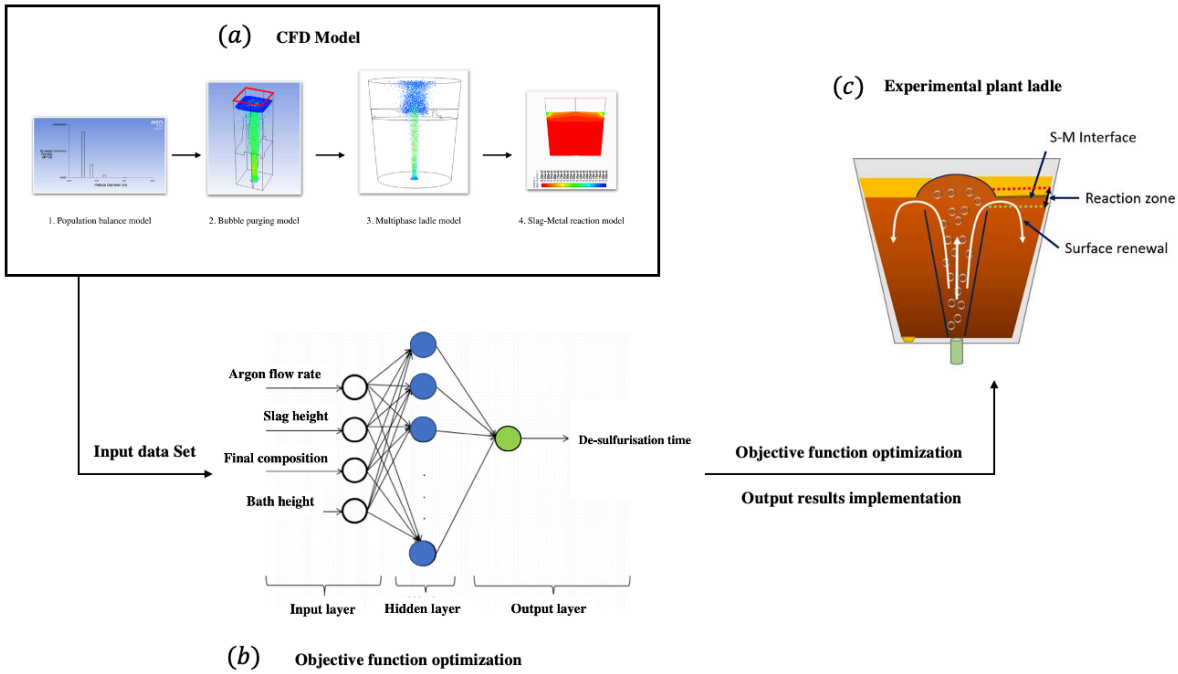

Fig 1: The pictorial representation of the overall process of Optimisation of a multi surrogate model system with the help of Genetic algorithm. (a) Represents the CFD model to obtain the input data set, (b) Represents the Neural network architecture for obtaining the Objective

1. anshs@iitk.ac.in

function, (c) Implementation of the optimised process variables in order to minimise the processing time.

B. Keywords: Surrogate models, ANN, Genetic Algorithm, Ladle furnace, productivity, process time, De-sulfurisation, Thermal, alloying, high grade steel.

C. Tentative topic: Multiphase CFD model based Machine learning model for de-sulfurization process in a ladle furnace. Genetic algorithm-ANN coupled optimisation for minimisation of ladle desulfurization time.

D. Theory:

Parallel and sequential operations in LF shows that there are numerous operations happening in LF at any point of time. Many of these runs in parallel. For example, arcing, purging, inclusion floatation and desulfurization can go on simultaneously. On the other hand, sampling and arcing cannot be done together. But sampling and purging can proceed together. So, there are numerous combinations. Broadly, the entire LF operation can be thought of three stages: refining stages I and II and trimming stage [4]. Overall reduction in LF processing time can therefore be associated to reduction in duration of these three stages. The time required for desulfurization, deoxidation (mainly inclusion floatation) and sampling require special attention. Slag preparation and alloying are other focus areas where there are possibilities of time reduction. Considering the complexity of the process, a detailed mathematical framework is needed to address the problem. The proposed mathematical framework is outlined in the next section.

The basic mathematical framework is based on five sub-modules:

(ii) Desulfurization (Thermodynamics and kinetics of desulfurization)

- **Introduction :**
- **Mathematical Models**
- **Results and Discussions**

(iii) Multi-phase flow model (To depict hydrodynamics inside ladle)

- **Introduction :**
- **Mathematical Models**
- **Results and Discussions**

The above timeline in Table 1 is made considering the major effects in the ladle processing, these are Tapping and subsequent addition of alloy and fluxes to make the initial slag. Thereafter the alloy melting and dissolution takes place with slag flux melting in situ. This serves as an example of a parallel process. Further, before the desulfurization can take place we need to first lower the bath oxygen level and after that, we need to change the property of the overlying slag in order to increase the basicity of this slag. After, slag modification is finished heavy argon purging is required in order to achieve better desulfurization (i.e slag-metal reaction) kinetics. This opens up paths for re-oxidation via slag eye and hence further inclusion removal is necessary prior to the final step of compositional alloy addition.

1. anshs@iitk.ac.in

Here we see that there are many parallel processes which happen together and some series processes which always happen separately. These are used in such a way to increase the efficiency of the overall refining. As for example, Desulfurization may take place with high oxygen content as well but that will be highly inefficient as the aluminum added (or any de-oxidizer will react preferentially with oxygen instead of taking part in the desulfurization reaction). After discussing the process summary above, we intend to discuss our process model and how the variables of these models affect our system. As in, the advantages and disadvantages of changing that process variable on the whole system. Since a single variable may affect more than one processes thus we may not obtain a single optimized solution for each variable. Here, we need to look at the plant-based objective function, which will be articulated in the later section.

The process variables which we have considered are Argon flow rate, Size of additions (alloys, fluxes, de-oxidisers, slag formers etc), Temperature of additions, Ladle length, Slag depth. The list is not exhaustive but in order to define the problem we have taken these variables based on their relative importance under our assumed conditions physical and process conditions of ladle processing.

Table 2: Process variables which we assume affect the ladle processing time

Process variable	**Functions**	
Argon flow rate:	• The Argon flow rate as being discussed affects melting as purging argon at room temp. Lowers the melt temperature. • It increases the de-O rate as more inclusions float up to the slag. • De-S kinetics increase as we increase the flow rate, which is due to increased slag-metal reaction. • Final stage inclusion floatation requires less purging as at the end the size of the inclusions are small.	Q
Size of additions:	• Increasing the size of additions increases the time required for their melting and dissolution • Whereas, increasing the size of addition lowers their manufacturing cost due to the law of comminution.	d_add
Temperature of additions:	• Increasing the temperature of additions lowers the time required for their melting and dissolution. • But it increases their input cost as pre-heating has got it's energy requirements.	T_add
Depth of slag:	• As the slag depth increases de-O and de-S increases as we may increase the purging rate with less re-oxidations from slag eye. • But subsequently, we get poor recovery and a much higher quantity of material is lost.	Ls

1. anshs@iitk.ac.in

	• This also increases the time taken for slag making and cost involved in raw materials for the slag	
Ladle length:	• Increasing the ladle length (keeping the volume constant) we may obtain a higher slag cover and the purging effect on slag metal reaction would increase. • De-Oxidation and inclusion floatation suffers as the residence time for these inclusions at the top of the bath and de-O products lower, thus the slag gets lesser time to catch them.	Ll

D.2 Objective function: To analyse this optimization we need to consider the plant-based objective function. We consider the case of an Integrated plant which aims at the completion of production levels more important than process cost but without negotiating with the quality.

The objective function is constructed according to the problem described in the initial paragraphs under the theoretical section.

With the advent of computational techniques, we can find these relations (connections) between these process objectives (processing time) and process variables through effective numerical modelling using the concepts of computational fluid dynamics. These models are mathematical representation of the actual physical processes under permissible assumptions. These complex models can be developed into efficient surrogate models such that the data from these full scale complex models can be used to generate simple surrogate models.

D.3 Time frames and corresponding models:

A: Thermal model, **B:** Hydrodynamics model, **C:** De-Sulfurization model, **D:** De-Oxidation model, **E:** Alloy melting and dissolution model. These models along with the Thermodynamic and kinetic fundamental models as discussed in table 3.

Table 3: Fundamental models of Thermodynamic and kinetic formulation in a multiphase steel-slag system.

Model	Governing physics	Results
Thermo-physical properties[5,6]	Slag-Metal Equilibration	Spatial and temporal Viscosity
Ladle hydrodynamics[2,8,9]	Mass and momentum conservation	Ladle furnace flow profile
Desulfurisation and Deoxidation reaction model[1,2,5]	Heterogeneous reaction in Eulerian Multi-phase setup	Composition profile in ladle
Bubble plume dynamics[8]	Discrete Phase modelling	Bubble size and spatial distribution
Slag-metal-bubble interaction[8]	Slag-Bubble interaction	Interfacial area and emulsification
Thermodynamic properties[4,5,7]	Slag-Metal Equilibration	Sulfide capacity, Activity coefficients.

1. Tapping **(t_1)** = constant
2. Heating of alloy + Slag-making **(t_2)** = A
3. De-O + Inclusion floatation **(t_3)** = D + B

1. anshs@iitk.ac.in

4. De-S Slag-making **(t_4)** = A
5. De-S **(t_5)** = C
6. Soft purging **(t_6)** = B
7. Final alloy addition, melting & homogenisation **(t_7)** = E + A + B

These surrogate models can be used to establish the relations between objectives (individual time frames, e.g., $\mathbf{t_{des}}$) and process variables (e.g Argon flow rate). These can be expressed as

$\mathbf{t_{des}} = \mathbf{t_4}$ = f1 (Q, L etc.)
$\mathbf{t_{slag\text{-}making}} = \mathbf{t_2} =$ f2 (T_addi , Size-addi etc.)

The surrogate models have certain advantage, as they adapt to the changes in the physical conditions much faster than the original models. (Show calculations between time comparison of surrogate and full-scale model) In this way the optimisation can be analysed and can be used in an on-line predictive control to maintain an optimal solution regardless of the changes in the physical conditions (e.g., Temp of new bath is 200 deg C less than previous, while tapping is taking place).

After the individual objective function are worked out, we will construct a net objective function
t_net = Σ ti , for all i's.

D.4 Factors affecting objective function:

First, we will do a qualitative analysis of the process variable and how they affect the factors of the ladle processing time. In the above flowcharts we see the effective relations and dependence of the variables upon each other. As stated, the overall process is very complex

D.5 Solution methodology:

The methodology to solve an optimisation problem is schematised in Fig. 3. The optimisation algorithm calls on the surrogate model to evaluate the decision variables and approximate the state variables (power output) which is fed to the objective function. The novelty of this method is that it relies solely on the surrogate model within the optimisation loop. This approach contrasts with previous studies [8, 13], which use the original simulation model to continually update the surrogate model as optimisation progresses. Therefore, our surrogate models 'stand-alone' and are not retrained according to the original 3D CFD model during optimisation. The benefit of this approach is enormously increased speed of optimisation.

1. anshs@iitk.ac.in

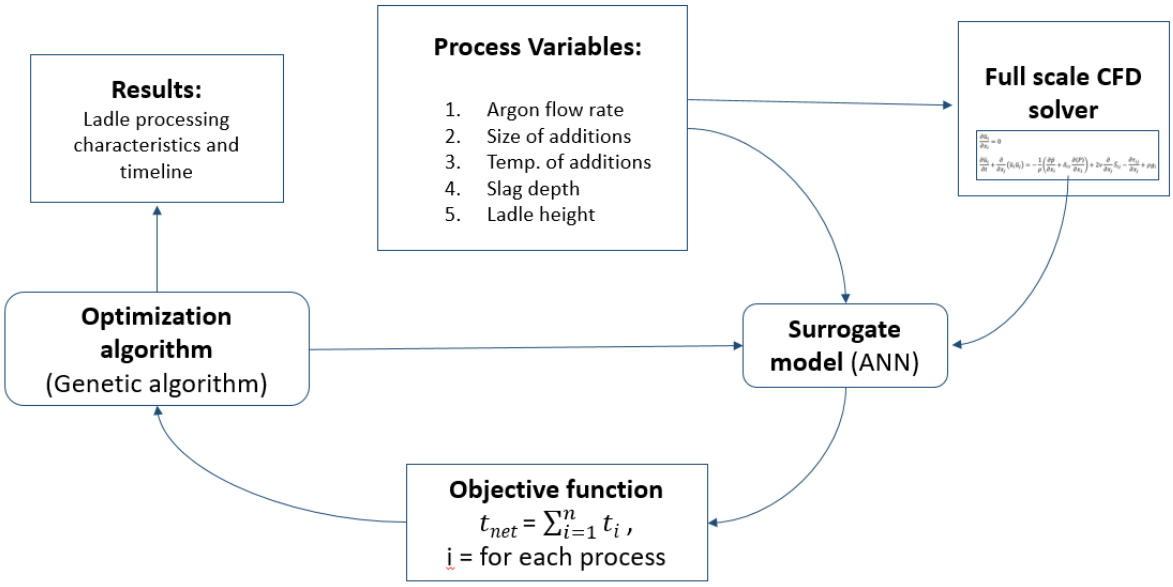

Fig 7: Flowchart of solution methodology.

D.6 Algorithm Steps:

1. Solve full scale CFD solver with appropriate BC and IC

2. Obtain data set from the full scale model, which captures the variations of all process variables

3. Transfer the data set obtained in step 2, to the ANN based surrogate model

4. Obtain an objective function using an appropriate regressor in terms of process variables (as defined in Table 2)

5. Transfer the objective function created in step 4, to the optimisation algorithm.

    a. Initialise the Genetic algorithm based on appropriate initial values of Pr. Variables
    b. Find the t_i for the given surrogate model
    c. Update the initial values to new set of values with the help of Surrogate model
    d. Go to 5 (b) and repeat till Global optimum is reached
    e. Print the obtained optimum process variable values.

6. Print results for the optimum ladle processing process variables.

1. anshs@iitk.ac.in

*The above algorithm is set up for the optimisation of a single Surrogate model, we now need to couple different surrogate models together and find a global optimum for all these models.

D.7 Surrogate model:

ANN: Artificial neural networks are among the most important soft computing methods, widely used for a great range of applications spanning across various scientific fields. This method is able to successfully predict the outcome of a process by using pairs of input and output data in a learning procedure. In fact, this method imitates the function of biological neurons, which receive inputs, process them, and generate a suitable output. The most common ANN model, namely MLP, has a structure containing various interconnected layers of neurons, starting from an input layer and ending at an output layer. The middle layers are called hidden layers, and their number is variable, depending on the size and the characteristics of each problem. Each neuron is connected by artificial synapses to the neurons of the following layer, and a weighting coefficient, or weight, is assigned to each synapse. The inputs for each neuron are multiplied by the weighting coefficient of the respective synapse, and then, they are summed; after that, the output from each neuron is generated by using an activation function, which usually is a sigmoid function, such as the hyperbolic tangent. The ANN model is created by a learning process, containing three different stages, i.e., training, validation, and testing. For each stage, a part of the total input/output data is reserved, most commonly 70%, 15%, and 15%, respectively. The learning process consists of the determination of suitable weight values according to real input/output data pairs and is an iterative process. This process is called error backpropagation, as the difference of the predicted and actual output is first computed in the output layer, and then, the error is propagated through the network in the opposite way, from the output to the input layer; after various iterations, or epochs, the network weights are properly adjusted so that the error is minimized. The training and validation stage both involve adjustment of the weights, and it is possible to stop the learning process if the error is not decreasing after some epochs, a technique that is named the early stopping technique. Finally, during the testing stage, the trained model is checked for its generalization capabilities by providing it with unknown data from the testing data sample. Usually, the Mean Squared Error (MSE) is used for the determination of model performance:

< Karkalos, Nikolaos E., et al. "A comparative study between regression and neural networks for modeling Al6082-T6 alloy drilling." Machines 7.1 (2019): 13.>

1. anshs@iitk.ac.in

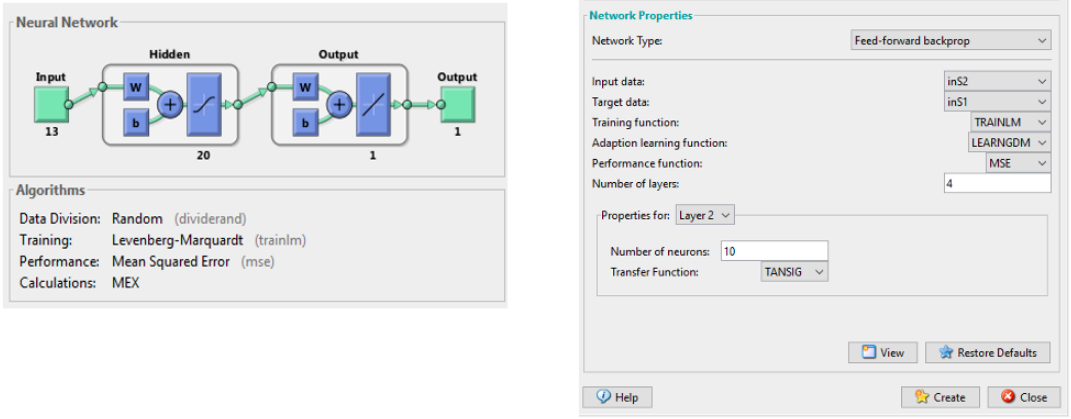

(a) (b)

Fig 8: (a)the implemented Matlab Neural network architecture, (b) Overview of the network used for the current NN training with the help of Matlab GUI.

With the NN model, we obtain the weights and biases which can be further used to predict any unknown test case. This way we can limit computation time

D.8 Optimization algorithm:

Evolutionary computation EC, a term devised only in the last two decades, represents a broad spectrum of heuristic approaches for simulating evolution Back et al. 2000. Primary examples include genetic algorithms GAs Holland 1962; Holland 1975, evolutionary strategies ES Rechenberg 1973; Schwefel 1981, evolutionary programming Fogel et al. 1966, and genetic programming Koza 1992. Collectively referred to as evolutionary algorithms EAs, these methods are comprised of algorithms that operate using a population of alternative solutions or designs, each represented by a potential decision vector. EAs rely on randomized operators that simulate mutation and recombination to create new individuals i.e., solutions who then compete to survive via the selection process, which operates according to a problem-specific fitness function Back et al. 2000. EA popularity is, at least in part, due to their potential to solve nonlinear, nonconvex, multimodal, and discrete problems for which deterministic search techniques incur difficulty or fail completely. The growing complexity and scope of environmental and water resources applications has served to expand EAs' capabilities. The objective of this paper is to critically review recent EC applications and the state-of-the-art, with particular focus on GAs given their dominant use in the historical literature of the water resources planning and management field. Conceptualized by ASCE's Task Committee on Evolutionary Computation in Environmental and Water Resources Engineering, this paper contributes a comprehensive resource for water resources researchers interested in applying EC and seeks to promote cross fertilization between the many areas of water related research where EAs are being applied.

1. anshs@iitk.ac.in

< Nicklow, John, et al. "State of the art for genetic algorithms and beyond in water resources planning and management." Journal of Water Resources Planning and Management 136.4 (2010): 412-432. >

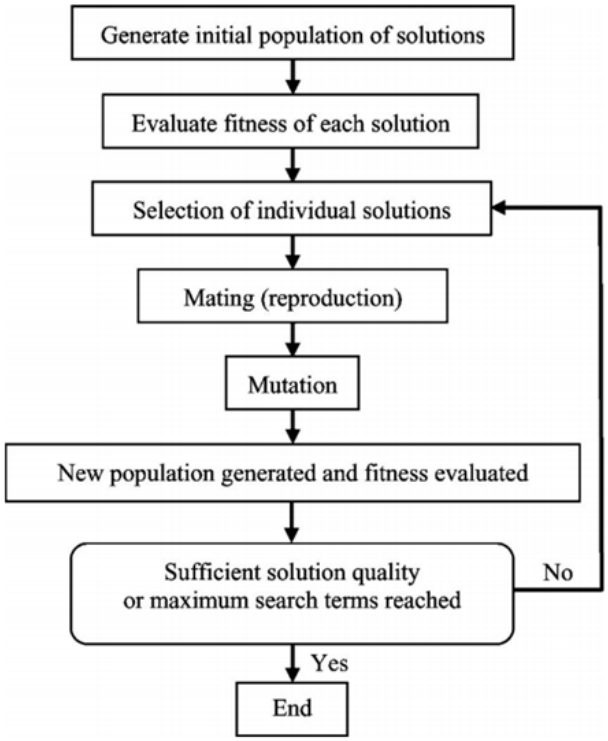

Fig 9: Structure of Genetic algorithm used in the current simulation

MLP features: In this study, **Levenberg-Marquardt (LM) learning algorithm** was used to adjust the weights in the multilayered feed-forward networks. In hidden layer, logistic sigmoid nonlinear function (logsig) and in output layer, linear transfer function (purelin) were used as an **activation function.**

Analysis of Multiple regression model (MSR): **<Work left>**

1. ANOVA Table
2. P value : The lower p value of co-effcients the more deterministic there values are
3. R2 value: R2 close to unity (coefficient of multiple determination)
4. Residual : to test the models' accuracy; in both cases, all points were positioned near to a straight line

Analysis of Multilayer perceptron model (MLP): **<Test results : Finalise>**

1. No. of Hidden Neurons
2. MSEtrain

1. anshs@iitk.ac.in

3. MSEtest
4. MAPEtrain (%)
5. MAPEtest (%)

*If MSE or MAPE first decreases and then increases while increasing the number of hidden neurons, then we observe an overfitting.

Convergence of target and model output values can be observed with the use of Mean Error (BIAS),

Mean absolute error (MAE),
Mean absolute percentage error (MAPE) and root mean square error (RMSE).
Analysis of Radial Basis Function Neural Network Models (RBF-NN)
Analysis of Adaptive Neuro-Fuzzy Inference System Models (ANFIS)

E. CFD Part < Check placement>

E.1 Model aim: In the present chapter we will be discussing the Multiphase Multi-species reaction ladle model, this includes the earlier discussed DPM model and the multiphase model along with the newly added component of species transport and reactions. This model will also come under the regime of Euler-Langrangian model. This model is a proper E-L model, since the species transport equation is an exclusive component which needs separate eulerian modelling. In this multiphase domain equations depicting the phase boundary is solved in order to include the surface phenomenons, this model is used to depict the partitioning of elements between slag and steel or rather transport of elements from metal to slag phase. The transport occurs the other way round as well, but since we will be focusing on the transport of 'Sulphur', which is deleterious to steel. Thus we will only be focusing on the transfer of this element from steel to slag.

E.2 Model description:

A fully transient 2D axisymmetric numerical model of was implemented using a combination of the discrete phase, volume of fluid multiphase and species transport models. The model describes the physical picture of an experimental ladle getting purged with argon gas and interactions between the slag and steel layer while the whole system is being agitated with a purging gas.

The steel slag reaction is set up as a species mass transfer model, for which appropriate UDF is written to describe the rate of this transfer. The mass transfer is then applied to the species transport term as a source term. More on this is discussed in Chapter

1. anshs@iitk.ac.in

For this simulation we have used the same mesh and multiphase setting.

E.3 Geometry:

FLUENT's standard pre-processor, design modeller was used to create and mesh the geometries. The 2D regime was created with dimensions required by the settings for the future experimental runs, ie. the diameter of the ladle is 1.2, with steel filled till 3.12m and a slag layer of depth 0.10 m with purging taking place with a 80 mm diameter purger.

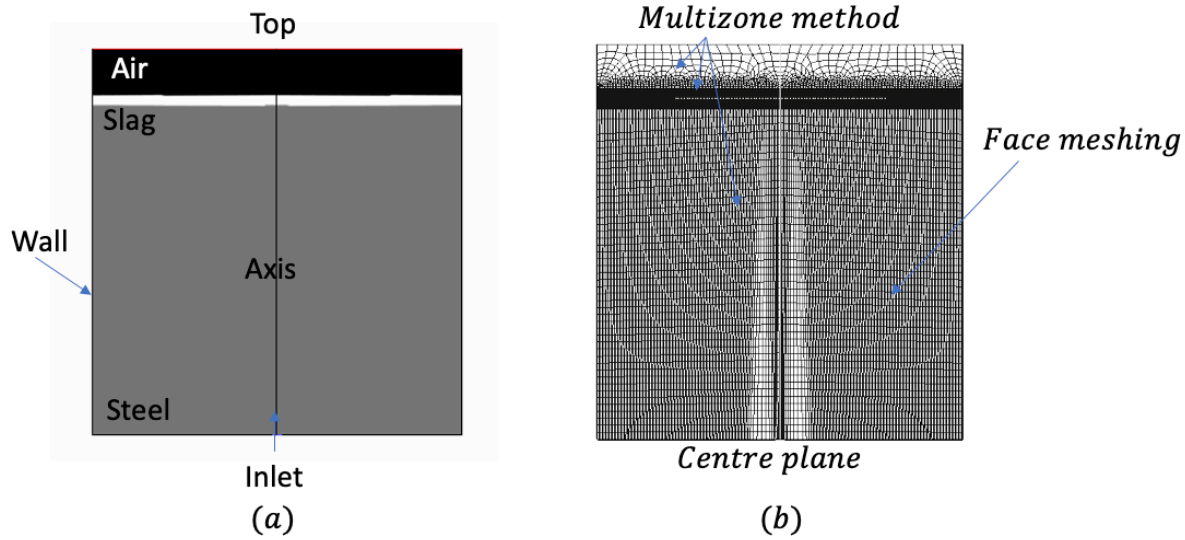

Fig 2: (a) Geometry and names of boundaries of the current numerical simulation and the 3 phases of the simulation in a 2-dimensional view of this geometry with water (grey), oil (white) and air (black). (b) Mesh used in the current computational study.

Methods: All Quads

After face meshing was used in the lower section of the mesh zone. But the top fine zone was left to triangle dominant meshing. We observe a very large number of nodes, which are all unstructured and due to which increase computation time.

Table 2 : Mesh Sizing

Attributes	**Value**
Size Function	Curvature
Relevance Center	Coarse
Initial Size Seed	Active Assembly

1. anshs@iitk.ac.in

Table 2 : Mesh Sizing

Attributes	Value
Span Angle Center	Fine
Curvature Normal Angle	Default (18.0 °)
Min Size	2.08e-003 m
Max Face Size	1.e-002 m
Growth Rate	Default (1.20)
Automatic Mesh Based Defeaturing	On
Defeature Size	1.04e-003 m
Minimum Edge Length	4.e-002 m

E.4 Governing equations:

The standard conservation equations for mass, momentum, species:

$$\frac{\partial \rho}{\partial t} + \nabla \cdot (\rho \vec{v}) = S_m$$

$$\frac{\partial}{\partial t}(\rho \vec{v}) + \nabla \cdot (\rho \vec{v}\,\vec{v}) = -\nabla p + \nabla \cdot (\bar{\bar{\tau}}) + \rho \vec{g} + \vec{F}$$

$$\frac{\partial}{\partial t}(\rho Y_i) + \nabla \cdot (\rho \vec{v}\, Y_i) = -\nabla \cdot \vec{J}_i + R_i + S_i$$

For a more detailed description, see Chapter 3.(Ch 3, Eq 3.2-4)

E.5 Multiphase modeling:

The multiphase model was implemented since the column had air above the water column. This was implemented using the volume of fluid model.

E.6 Volume of fluid:

In the current work, the mathematical model is based on the Eulerian multiphase approach. In the current model multiple phases are Water (Primary) and Air phase (Secondary) The continuity equation for phase q can be written as: (Ch 3, Eq 7-8)

1. anshs@iitk.ac.in

$$\frac{\partial}{\partial t}(\alpha_q \rho_q) + \nabla \cdot (\alpha_q \rho_q \vec{u}_q) = 0$$

where,

α_q = the volume fraction of phase 'q'

ρ_q = density of phase 'q'

$\vec{u}_q$ = velocity of the 'q' th phase.

$$\frac{\partial}{\partial t}(\alpha_q \rho_q \vec{u}_q) + \nabla \cdot (\alpha_q \rho_q \vec{u}_q \vec{u}_q) = -\alpha_q \nabla p + \nabla \cdot \bar{\tau}_q + \alpha_q \rho_q \vec{g} + \vec{F}_{drag,q} + \vec{F}_{lift,q} + \vec{F}_{VM,q}$$

E.6 Discrete phase model:

The Argon gas bubbles which are being purged in the ladle is modelled as discrete phase particles. The detailed discussion on modelling of bubbles in a fluid system is discussed in Model III and the detailed discussion on the DPM modelling technique is discussed in the Chapter on CFD theory. With that discussion we hereby, present the equations governing the trajectory of the bubbles(particles) and the numerical strategy which we have followed while modelling the Bubble flow in a Metallurgical Ladle. (Ch

$$\frac{d\vec{u}_p}{dt} = F_D(\vec{u} - \vec{u}_p) + \frac{\vec{g}(\rho_p - \rho)}{\rho_p} + \vec{F}$$

$$Re \equiv \frac{\rho d_p \left| \vec{u}_p - \vec{u} \right|}{\mu} \qquad F_D = \frac{18\mu}{\rho_p d_p^2} \frac{C_D Re}{24}$$

3, Eq 3.10-12)

As described in the previous chapter, these equations govern the trajectory of the particles by solving the above Ordinary differential equations along with its source term. The main challenge which one faces is to model the coefficients and the source term in this equation, since now we are describing a phenomenon using this equation. Henceforth appropriate changes are required.

These terms change with the type of physical models they are being represented for. One example of different physical system may be modelling single bubble versus

1. anshs@iitk.ac.in

modelling a swarm of bubbles in a quiescent media. One other example may be to model a spherical bubble versus modelling a capped bubble. Henceforth, the appropriate models for the coefficients is necessary to contain the physics in these equations.

Here, we will be following the same modelling approach as we have already discussed. However the DPM initial conditions would change with the change in the system's physical condition. Since, we are now operating with a different flow rate and a different kind of purger dimension hence we need to take care of that in our model. This will be discussed in the following section, which covers the physical properties and the boundary conditions of the Discrete phase along with the continuous phase.

3.2.5.9 Turbulence flow modeling:

The standard k-e model was implemented to model turbulence inside the ladle. The default values of the constants were implemented as . The turbulence parameter of DPM particles were also included, turbulent dispersion within the plume in the absence of a generalised model for turbulence modulation by the rising bubbles. Detailed picture about this modelling is discussed in previous section on turbulence modelling.

3.2.5.10 Reaction modelling/ Source term modelling :

The species transport equation as discussed in the governing equations needs to be modelled to accommodate the chemical reaction. The chemical reaction among species produces products and at the same time consumes the reactants. These reactants and products may come from the same phase or different phases, when they belong to different phase the setup comes under the regime of heterogeneous reaction. These reactions can be modelled in several ways, in this chapter we have employed the mass transfer approach, i.e [2]

- transport of reactant to the interface,
- simultaneous reaction and
- further transport of products.

1. anshs@iitk.ac.in

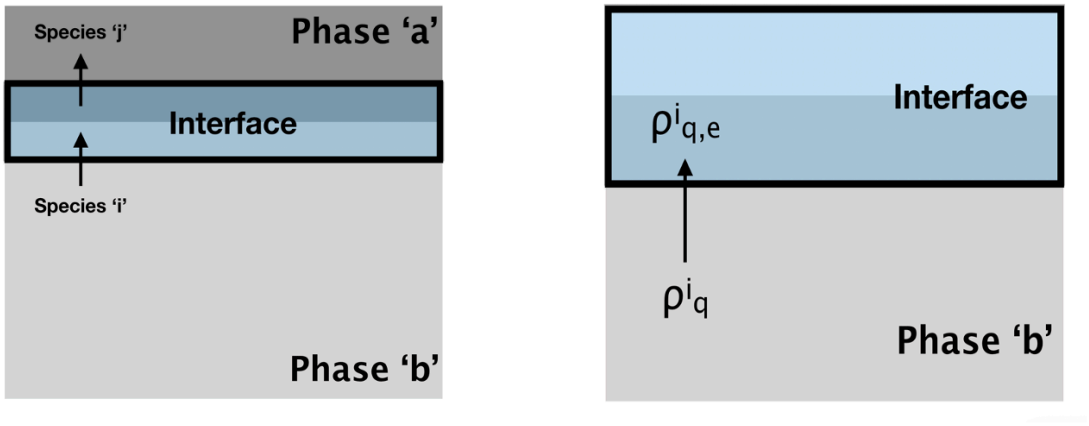

(a) (b)

Fig 5: (a) Showing the mechanism of interfacial reaction between two phases. Species 'i' represent species getting depleted from the Phase 'b' and Species 'j' represents species getting added in Phase 'a'. (b) Fig 6: The potential across which bulk species ρ_q^i will from towards the interface. Given that the equilibrium concentration at the surface '$\rho_{q,e}^i$' is lower than the bulk concentration ρ_q^i.

This source the is actually written as a sink term, i.e the term which denotes the exit of all such mass fraction 'Y_i' from phase 'q' to all the other phases (n phases in total), here we only have a single phase 'p' = slag, where the solute will go.

$$S_i = \dot{m}_{p^i q^i} = k_{pq} a_i \left(\rho_{q,e}^i - \rho_q^i \right), \tag{3}$$

The formulation of mass transfer co-efficient 'k_{pq}' requires knowledge about flow field and properties flowing materials. In this work mass transfer co-efficient is formulated through 'small eddy theory' which has been discussed in detail in the 7th Chapter of this thesis. Simply reviewing that discussion we can say, the difference can be written as difference of concentration between the species present at the interface '$\rho_{q,e}^i$' and concentration of species present in the bulk of the liquid 'ρ_q^i ' ! We have already assumed that the chemical reaction is invariably were fast, probably due to the high temperatures pertaining to the molten steel slag interface in the ladle. Thus the concentration at the interface will set up to an equilibrium concentration before the species transport physics can know about the change! Henceforth we can safely write the interfacial concentration as the equilibrium concentration only. The 'a_i' is the area density pertaining to the interface of the reaction.

1. anshs@iitk.ac.in

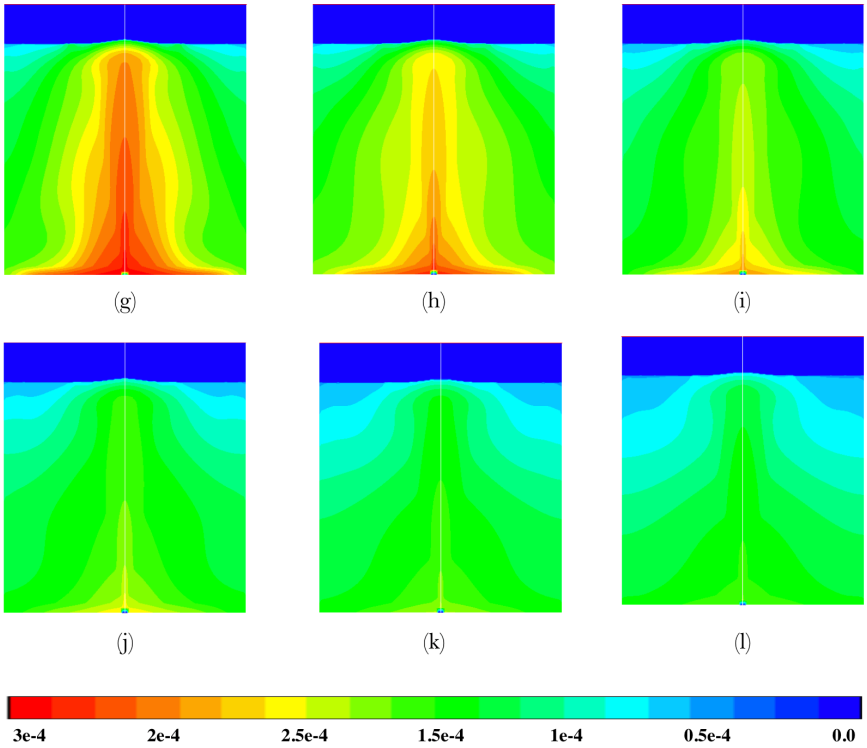

Fig 4.4.11: Contour plots after 30 seconds. From fig (g) after 210 sec , fig (h) after 240 sec, fig (i) after 270 sec, fig (j) after 300 sec, fig (k) after 330 sec, fig (l) after 360 sec.(purging rate = 80 NLm).

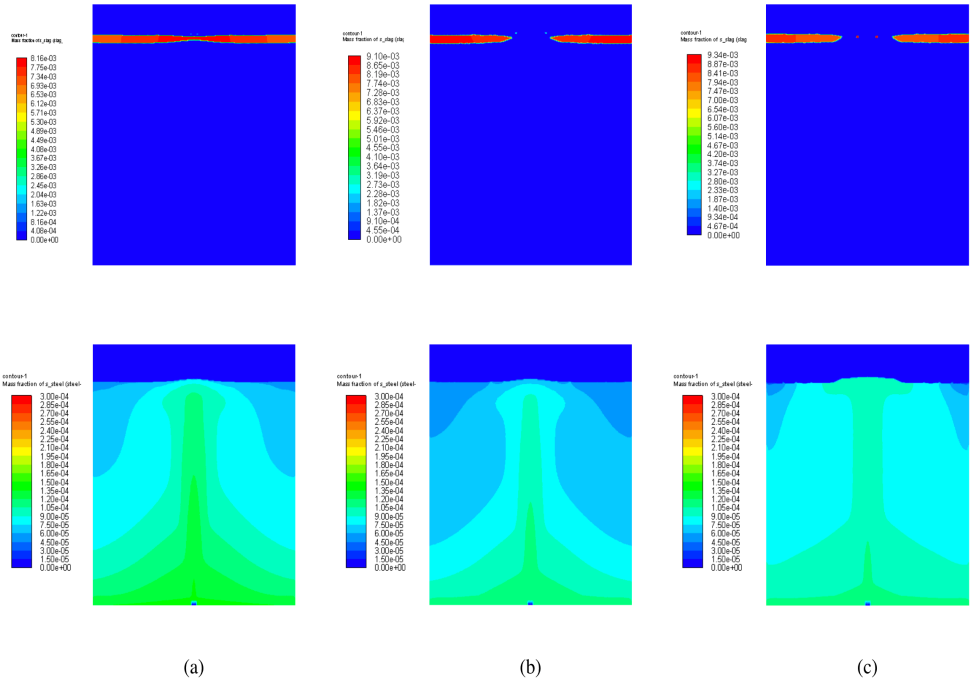

1. anshs@iitk.ac.in

Fig 4.4.14: Contour plots of mass fraction in saga phase and metal phase after 480 seconds. fig (a) at 80 NLm, (b) at 200 NLm, (c) at 400 NLm.

References:

[1] 1. Andersson, Margareta, et al. "Slag-metal reactions during ladle treatment with focus on desulphurisation." Ironmaking & steelmaking 29.3 (2002): 224-232.
[2] Singh, Umesh, et al. "Multiphase modeling of bottom-stirred ladle for prediction of slag–steel interface and estimation of desulfurization behavior." Metallurgical and Materials Transactions B 47.3 (2016): 18041816
[3] Liu, Yu, et al. "A Review of Physical and Numerical Approaches for the Study of Gas Stirring in Ladle Metallurgy." Metallurgical and Materials Transactions B 50.1 (2019): 555-577.
[4] Richardson, F. D., and C. J. B. Fincham. "Sulphur in silicate and aluminate slags." Journal of the Iron and Steel Institute 178.1 (1954): 4-15.
[5] Ghosh, Ahindra. Secondary steelmaking: principles and applications. CRC Press, 2000.
[6] PG, Jönsson, Lage Jonsson, and Du Sichen. "Viscosities of LF slags and their impact on ladle refining." ISIJ international 37.5 (1997): 484-491.

ANNEXURE:

Training data sets from full CFD model.

Table 4.1: Training Data-Set 2 obtained from desulphurisation from CFD solver

Q_dot	L	dL	Si	Sf	t_des
100	1.8	0.1	80	10	14
80	1.8	0.1	80	10	16
120	1.8	0.1	80	10	10
140	1.8	0.1	80	10	8
160	1.8	0.1	80	10	7
100	1.6	0.1	80	10	15
100	1.4	0.1	80	10	14
100	2	0.1	80	10	10
100	2.1	0.1	80	10	8

Table 4.2: Training Data-Set 2 obtained from desulphurisation from CFD solver

Time		S1	S2	S3	Mass fraction	% wt
0	**0**	3.00E-04	3.00E-04	3.00E-04	3.00E-04	3.00E-02

1. anshs@iitk.ac.in

30	**0.5**	2.15E-04	3.00E-04	3.00E-04	2.72E-04	2.72E-02
60	**1**	1.80E-04	2.75E-04	3.00E-04	2.52E-04	2.52E-02
90	**1.5**	1.65E-04	2.25E-04	2.85E-04	2.25E-04	2.25E-02
120	**2**	1.60E-04	2.10E-04	2.65E-04	2.12E-04	2.12E-02
150	**2.5**	1.55E-04	1.95E-04	2.45E-04	1.98E-04	1.98E-02
180	**3**	1.50E-04	1.80E-04	2.25E-04	1.85E-04	1.85E-02
210	**3.5**	1.37E-04	1.72E-04	1.95E-04	1.68E-04	1.68E-02
240	**4**	1.23E-04	1.64E-04	1.78E-04	1.55E-04	1.55E-02
270	**4.5**	1.20E-04	1.50E-04	1.70E-04	1.47E-04	1.47E-02
300	**5**	1.10E-04	1.46E-04	1.62E-04	1.39E-04	1.39E-02
330	**5.5**	1.06E-04	1.38E-04	1.52E-04	1.32E-04	1.32E-02
360	**6**	1.02E-04	1.30E-04	1.43E-04	1.25E-04	1.25E-02
390	**6.5**	1.00E-04	1.20E-04	1.33E-04	1.18E-04	1.18E-02
420	**7**	9.21E-05	1.15E-04	1.25E-04	1.11E-04	1.11E-02
450	**7.5**	8.31E-05	1.11E-04	1.20E-04	1.05E-04	1.05E-02
480	**8**	7.60E-05	1.05E-04	1.13E-04	9.79E-05	9.79E-03
510	**8.5**	6.90E-05	9.71E-05	1.17E-04	9.44E-05	9.44E-03
540	**9**	6.60E-05	9.01E-05	1.10E-04	8.87E-05	8.87E-03
570	**9.5**	6.24E-05	8.27E-05	1.01E-04	8.21E-05	8.21E-03
600	**10**	5.95E-05	7.80E-05	9.61E-05	7.79E-05	7.79E-03
630	**10.5**	5.93E-05	7.58E-05	9.12E-05	7.55E-05	7.55E-03
660	**11**	5.91E-05	7.20E-05	8.71E-05	7.27E-05	7.27E-03
690	**11.5**	5.88E-05	6.85E-05	8.15E-05	6.96E-05	6.96E-03
720	**12**	5.86E-05	6.25E-05	7.67E-05	6.60E-05	6.60E-03
750	**12.5**	5.85E-05	6.04E-05	7.62E-05	6.50E-05	6.50E-03
780	**13**	5.84E-05	5.97E-05	7.10E-05	6.31E-05	6.31E-03
810	**13.5**	5.82E-05	5.90E-05	6.50E-05	6.08E-05	6.08E-03
840	**14**	5.81E-05	5.86E-05	6.01E-05	5.89E-05	5.89E-03
870	**14.5**	5.81E-05	5.84E-05	5.90E-05	5.85E-05	5.85E-03
900	**15**	5.80E-05	5.83E-05	5.85E-05	5.83E-05	5.83E-03

Table 4.3: Training Data-set 3 obtained from desulphurisation from CFD solver

Q_dot	**L**	**dL**	**si**	**sf**	**ds**	**t_des (min)**
70	3.26	0.01	0.03	0.0102	0.0198	10
70	3.26	0.01	0.03	0.01126	0.0205	9

1. anshs@iitk.ac.in

70	3.26	0.01	0.03	0.012732	0.02062	8
70	3.26	0.01	0.03	0.01415	0.0207	7
70	3.26	0.01	0.03	0.017732	0.02079	6
70	3.26	0.01	0.03	0.0192	0.0209	5
70	3.26	0.01	0.03	0.0212	0.02108	4
70	3.26	0.01	0.03	0.02321	0.021173	3
70	3.26	0.01	0.03	0.024504	0.02125	2
70	3.26	0.01	0.03	0.027041	0.021311	1
80	3.26	0.01	0.03	0.0095	0.0205	10
80	3.26	0.01	0.03	9.87E-03	0.020126	9
80	3.26	0.01	0.03	1.13E-02	0.018702	8
80	3.26	0.01	0.03	1.31E-02	0.016879	7
80	3.26	0.01	0.03	1.45E-02	0.015485	6
80	3.26	0.01	0.03	1.63E-02	0.01371	5
80	3.26	0.01	0.03	1.95E-02	0.0105	4
80	3.26	0.01	0.03	2.20E-02	0.008015	3
80	3.26	0.01	0.03	2.41E-02	0.00588	2
80	3.26	0.01	0.03	2.62E-02	0.0038	1

1. anshs@iitk.ac.in